

Supporting Information

**2,3-Diaminophenazine@carbon felt with chemical grafting via amide bonds as an electrode in lithium-ion
batteries**

Peimeng Qiu^a, Yi Li^a, Hongquan Wang^a, Daoyu Li^b, Shengping Wang^{a,*}, Jingxian Yu^{c,*}

^a Faculty of Materials Science and Chemistry, China University of Geosciences, Wuhan 430074, China

^b Guiyang Bureau, Extra High Voltage Power Transmission Company, China Southern Power Grid (CSG), Guiyang 550081, China

^c ARC Centre of Excellence for Nanoscale BioPhotonics (CNBP), School of Chemistry and Physics, The University of Adelaide, Adelaide, SA 5005, Australia

* Corresponding Author. spwang@cug.edu.cn, jingxian.yu@adelaide.edu.au

1 Experimental

1.1 Material preparation

The carbon felts (6 mm thickness) before acidification were dried at 100 °C under vacuum for 10 h, cut into discs of 12-mm diameter, immersed in a mixed acid of HNO₃/H₂SO₄ (1/3 volume ratio) at 99 °C for 6 h. The acidified carbon felts were rinsed several times with distilled water until neutral and dried under vacuum at 100 °C for 48 h. The acidified carbon felts (C) were soaked in an N-methyl-2-pyrrolidone (NMP) solution of 2,3-diaminopheazine (DAP) at a concentration of 30 mg mL⁻¹ for 24 h, removed, and dried at 65 °C under vacuum for 24 h. The DAP@C composite materials were obtained. The DAP@C materials were used directly as the test electrodes. The load of DAP was ~0.53 mg cm⁻².

1.2 Electrochemical measurements

The DAP electrodes were prepared by casting well-homogenized slurries of DAP, Super P, and polyvinylidene fluoride binder with a ratio of 5:4:1 (wt %) in NMP onto aluminum foil. After solvent evaporation, the electrodes were cut into discs with a diameter of 12 mm and dried thoroughly in a vacuum oven at 65 °C for 24 h. The load of DAP was ~1.33 mg cm⁻².

All coin batteries for the electrochemical measurements were assembled in an argon-filled glove box with oxygen and moisture levels below 0.5 ppm. The batteries were assembled with DAP or DAP@C as the working electrode, lithium foil as the counter electrode, a Celgard 2400 membrane as the separator and 1 M LiPF₆ dissolved in ethylene carbonate (EC) and dimethyl carbonate (DMC) (1:1 volume ratio) as the electrolyte.

Galvanostatic charge/discharge measurements with 1.5–3.2 V at 0.1 A g⁻¹ of the test batteries were tested on a BT2000 Arbin battery test system. Cyclic voltammogram (CV) data were recorded at a scan rate of 0.1 mV s⁻¹ in the voltage range of 1.5–3.2 V on a VMP3 electrochemical workstation. The electrochemical impedance spectroscopy (EIS) spectrum was obtained using a VMP3 electrochemical workstation with an alternating current signal amplitude of 5 mV in the frequency range of 10⁵–10⁻² Hz.

All electrochemical tests were performed at 25 °C.

1.3 Material characterizations

The chemical structures of the acidified carbon felt, DAP powder and DAP@C were characterized using a Nicolet 6700 Fourier transform infrared (FTIR) spectrometer, and their thermal properties were evaluated by thermogravimetric analysis (TGA). TGA was performed on an STA 409 PC simultaneous thermal analysis instrument from ambient temperature to 800 °C in a nitrogen atmosphere with a heating rate of 10 °C min⁻¹. The morphologies and microstructures of the samples were recorded using an SU8010 ultrahigh-resolution scanning electron microscope (SEM).

1.4 Computational details

The geometries of DAP were optimized in the gas phase at the B3LYP level of theory and 6-31+G (d, p) basis sets using the Gaussian 09 package to obtain the lowest energy and most stable molecular conformation of DAP. X (x = 1, 2) mol lithium ions, inserted into the above optimal DAP and optimizing structures under the same basis sets,

obtained the most stable molecular structure of DAP-Li and DAP-2Li. The keyword pop=npa was added to obtain the natural population analysis with natural bond orbital (NBO) theory, which showed the electron population in the compound and revealed the interactions between Li and DAP.

The Multiwfn 3.6 package was used to read the .fch file and perform the molecular van der Waals electrostatic potential distribution, and finally, the molecule ESP was presented by the visual molecular dynamics (VMD) package.

2 Calculation of the contribution ratio of diffusion and capacitance

By establishing the relationship between the peak current (i) and scan rate (v), the capacitive and diffusion-limited kinetics can be analyzed by using empirical equations.

$$i = av^b \quad (S1)$$

$$\ln i = b \times \ln v + \ln a \quad (S2)$$

where a and b are the adjustable parameters. Parameter b can be obtained from the slope of the linear relationship between $\ln i$ and $\ln v$. The b value of 1 indicates a capacitive process, while the b value of 0.5 represents a diffusion-controlled process.

Furthermore, qualitative analysis was performed to determine the contribution ratios between the two mechanisms at various scan rates based on the following equations.

$$i = k_1v + k_2v^{1/2} \quad (S3)$$

$$i / v^{1/2} = k_1v^{1/2} + k_2 \quad (S4)$$

where k_1v and $k_2v^{1/2}$ represent the surface capacitive effects and diffusion-controlled process, respectively. The parameters k_1 and k_2 are determined from the linear relationship of $i / v^{1/2}$ and $v^{1/2}$ based on Equation S4. The ratio of the area of the $k_1v \sim E$ curve to the area of the CV curve is the capacitance contribution ratio at a specific scan rate.

3 Lithium-ion diffusion coefficient

3.1 CV

The diffusion coefficients of lithium ions (D_{Li^+}) were calculated by the Randles-Sevcik equation with the peak currents obtained at various scan rates.

$$I_p = 2.69 \times 10^5 n^2 A D_{Li^+}^{1/2} C_{Li^+}^* v^{1/2} \quad (S5)$$

where I_p is the peak current (A), v is the scanning speed ($V s^{-1}$), n is the number of transferred electrons, A is the area of the electrode (cm^2), D_{Li^+} is the diffusion coefficient of lithium ions ($cm^2 s^{-1}$), and $C_{Li^+}^*$ is the volume concentration of lithium ions in the electrode ($mol cm^{-3}$). D_{Li^+} can be calculated from the slope of the linear relationship between I_p and $v^{1/2}$.

3.2 EIS

The Warburg coefficient σ can be obtained from the slope of the linear relationship between Z_{Re} and $\omega^{-0.5}$.

$$Z_{Re} = R_{\Omega} + R_{ct} + \sigma \omega^{-0.5} \quad (S6)$$

where Z_{Re} is the real part of the Nyquist plot, R_{Ω} is the internal resistance, R_{ct} is the charge transfer impedance, and ω is the angular frequency in the low frequency region.

The Li^+ diffusion coefficient (D_{Li^+}) is calculated using the above Warburg coefficient σ .

$$D_{\text{Li}^+} = \frac{R^2 T^2}{2 A^2 F^4 \sigma^2 C^2} \quad (S7)$$

where R is the gas constant ($8.314 \text{ J mol}^{-1} \text{ K}^{-1}$), T is the absolute temperature (298.5 K), A is the contact area of the electrode (cm^2), F is the Faraday constant (96485 C mol^{-1}), and C is the concentration of Li^+ (mol cm^{-3}).

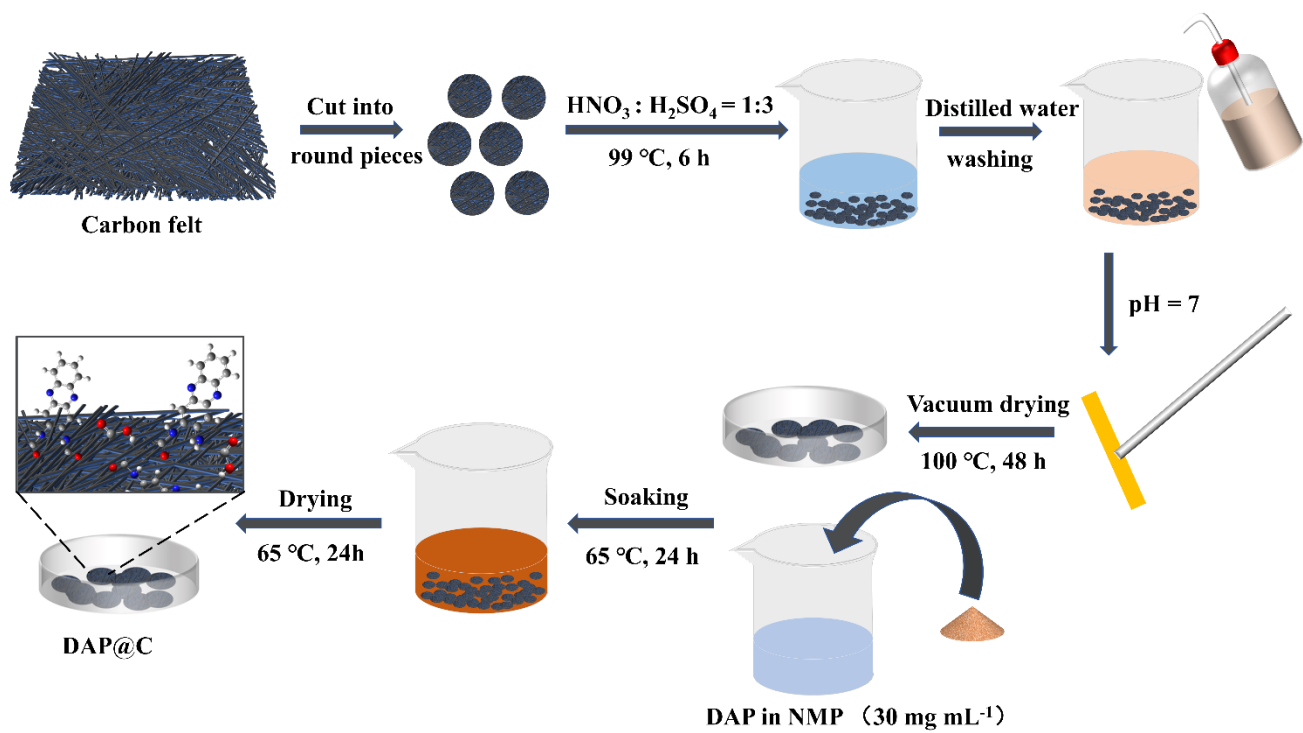


Figure S1 Preparation of DAP@C composites.

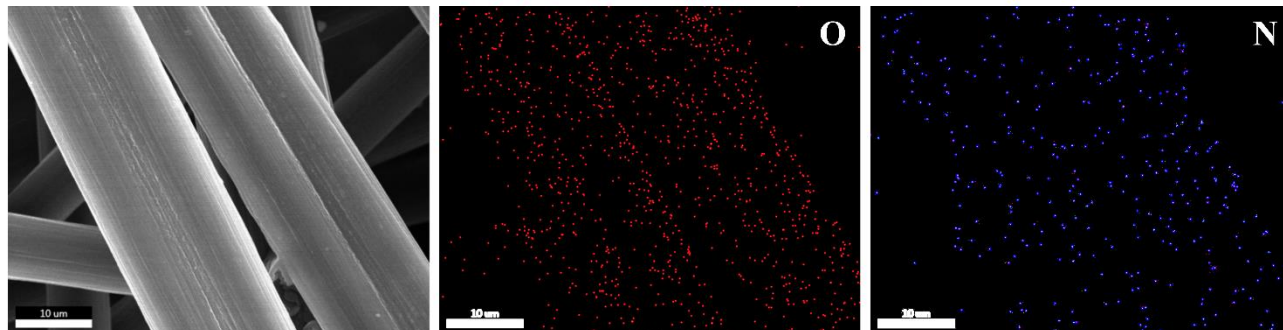


Figure S2 EDS maps of DAP@C.

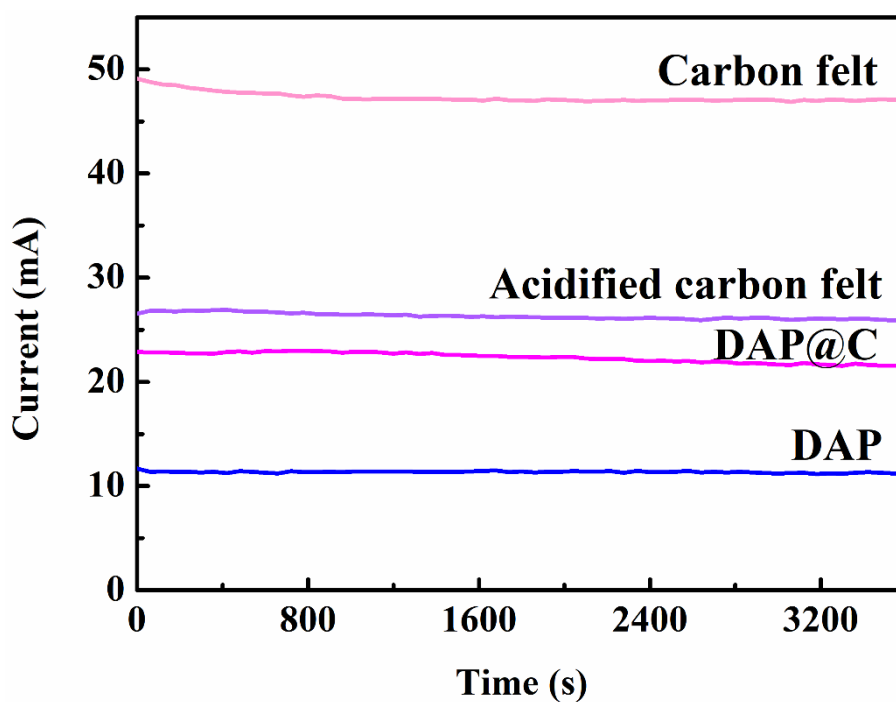


Figure S3 Electronic conductivity diagram of carbon felt, acidified carbon felt, DAP@C and DAP.

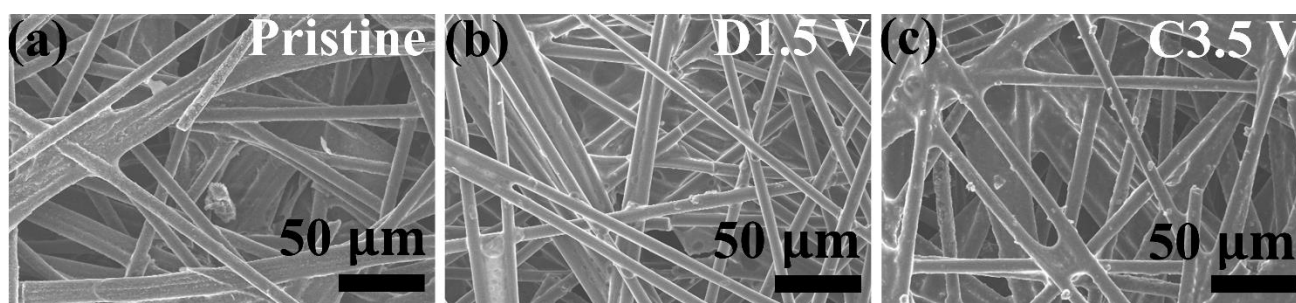


Figure S4 SEM images of DAP@C.

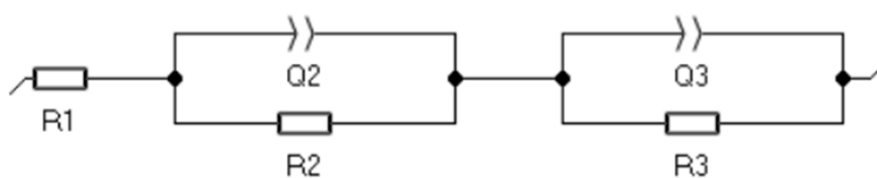


Figure S5 Equivalent circuit diagram. R1, R2, and R3 represent the ohmic impedance, the charge transfer impedance of the interface reaction, and the Warburg impedance, respectively, and Q2 and Q3 are the capacitance values.

In general, the semicircle of the EIS reflects the charge transfer impedance (R_{ct}) during electrochemical reactions, with a larger radius of the semicircle indicating a more difficult charge transfer. The slope of the tail in the low frequency region reflects the diffusion of lithium ions in the electrode.

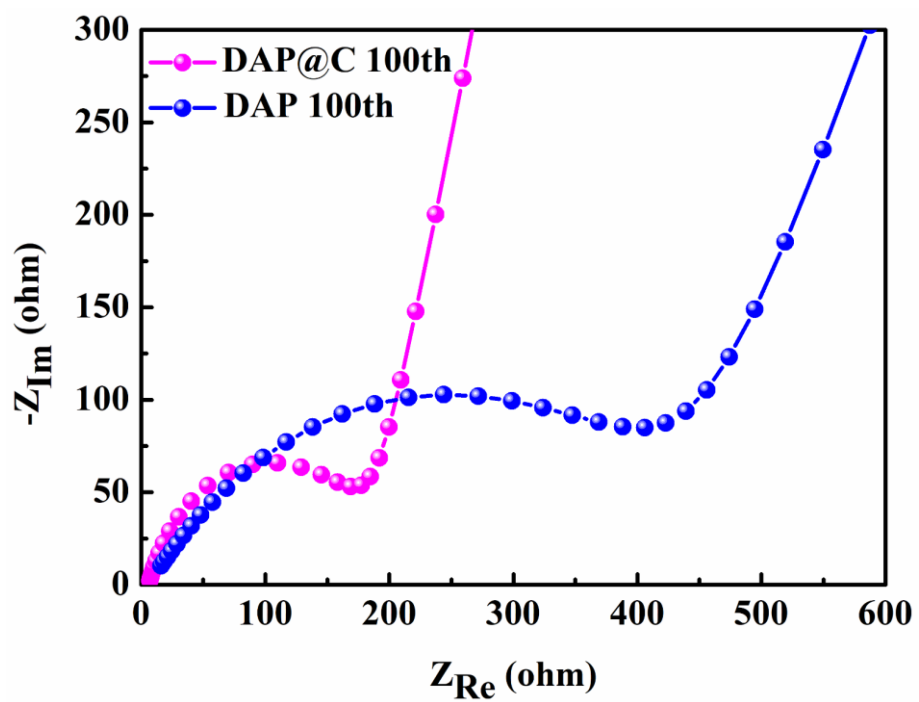


Figure S6 EIS spectra of DAP@C and DAP electrodes after 100 cycles.

The area of the redox peaks increased as the scan rate increased, showing a pair of strong redox peaks and a pair of weaker oxidation shoulder peaks, indicating that DAP@C was mainly a two-step single-electron reaction. The electrochemical properties of DAP@C are related not only to the molecular structure and C=N activity, but also to the reaction kinetics.

To further quantify the contribution of capacitive and diffusion control to the total capacity, the total current response (i) at a specific potential (V) can be divided into a capacitive control process (k_1v) and a diffusion control process ($k_2v^{1/2}$). The k_1 and k_2 constants are determined according to eqn (S4) to distinguish between capacitive and diffusive currents.

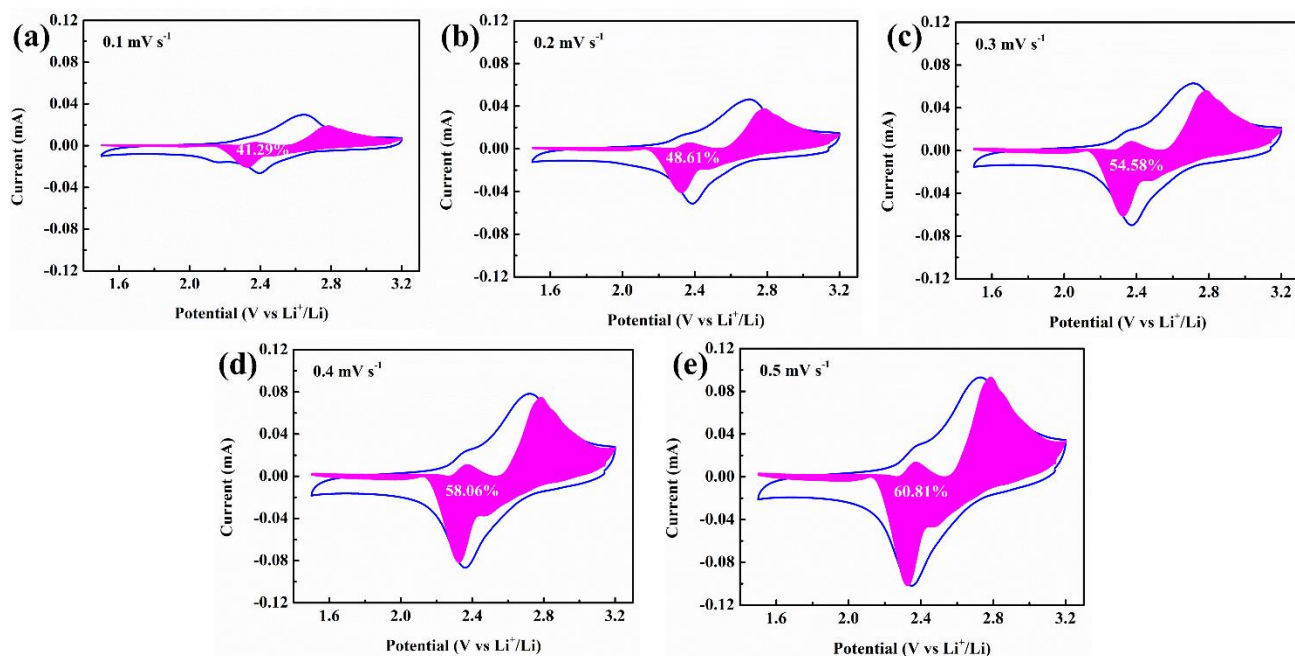


Figure S7 The percentage of capacitance contribution at various scan rates of DAP@C.

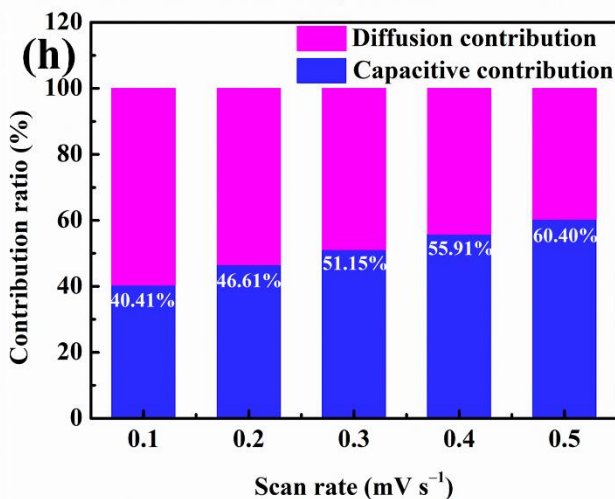
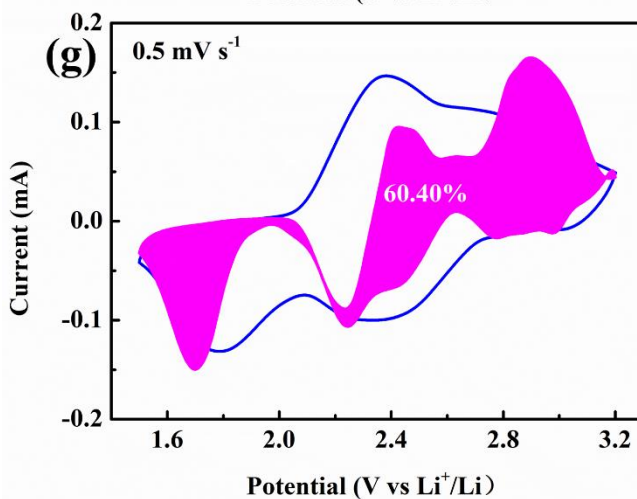
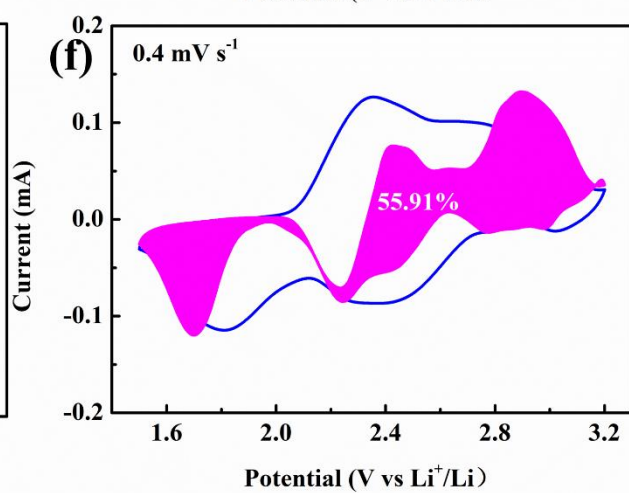
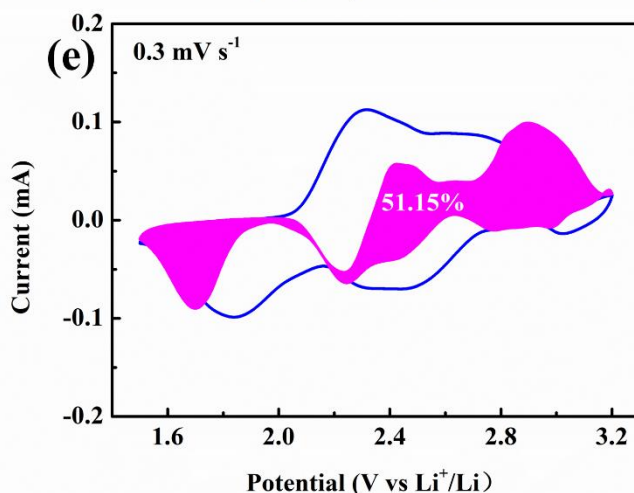
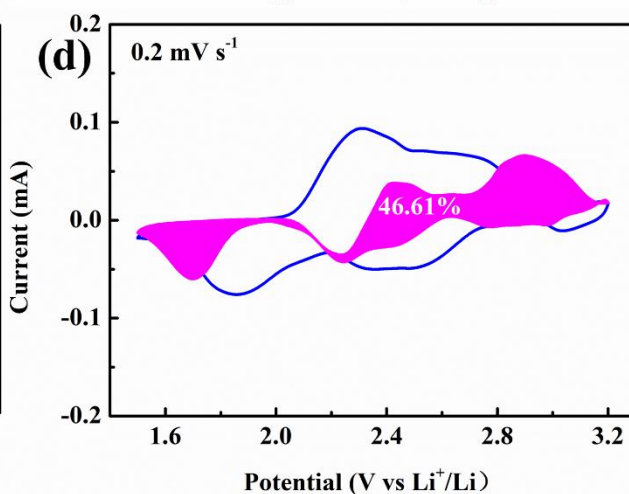
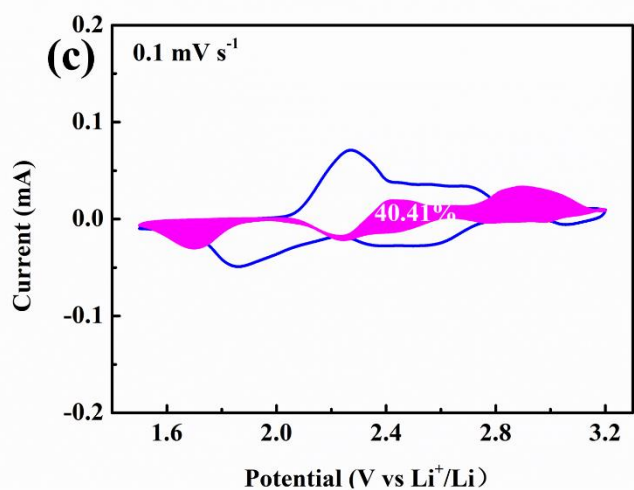
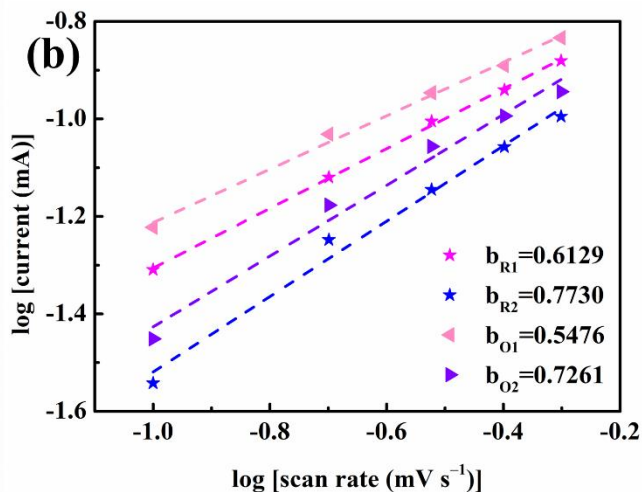
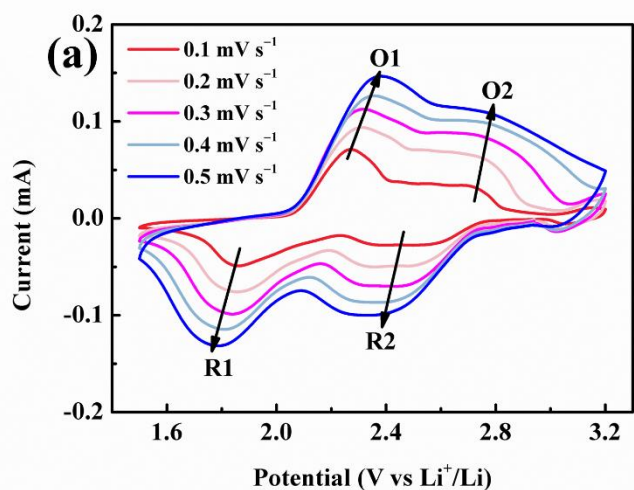


Figure S8 (a) CV curves at various scan rates, (b) corresponding relationship between peak current and scan rate of CV curves, (c-h) the percentage of capacitance contribution at various scan rates of DAP.

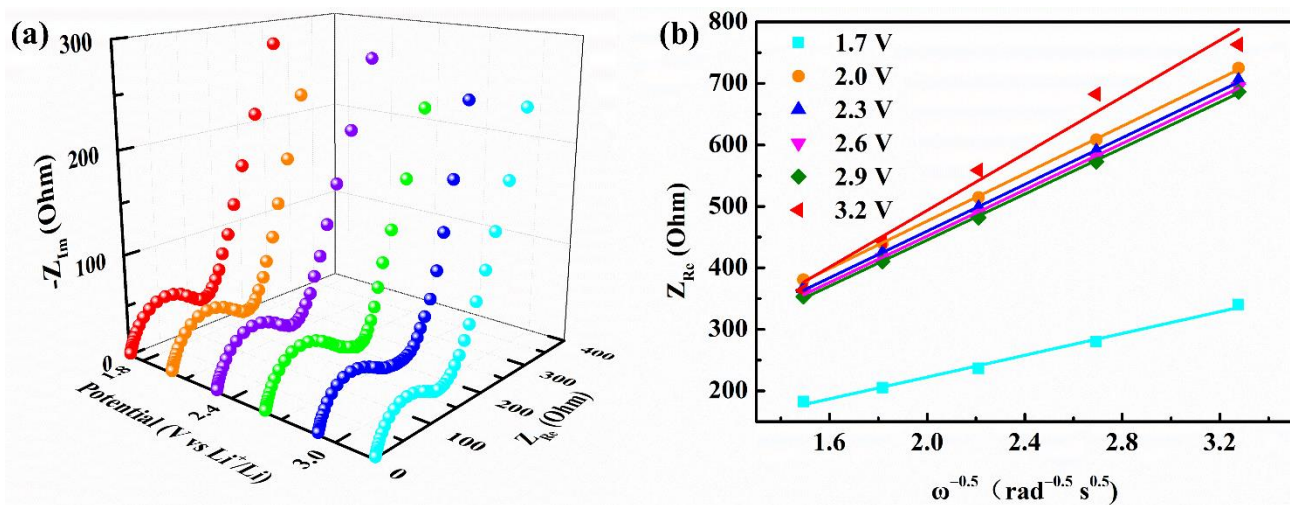


Figure S9 (a) EIS spectra at various charge potentials, (b) corresponding linear relationship between Z_{Re} and $\omega^{-0.5}$ of DAP@C during charging.

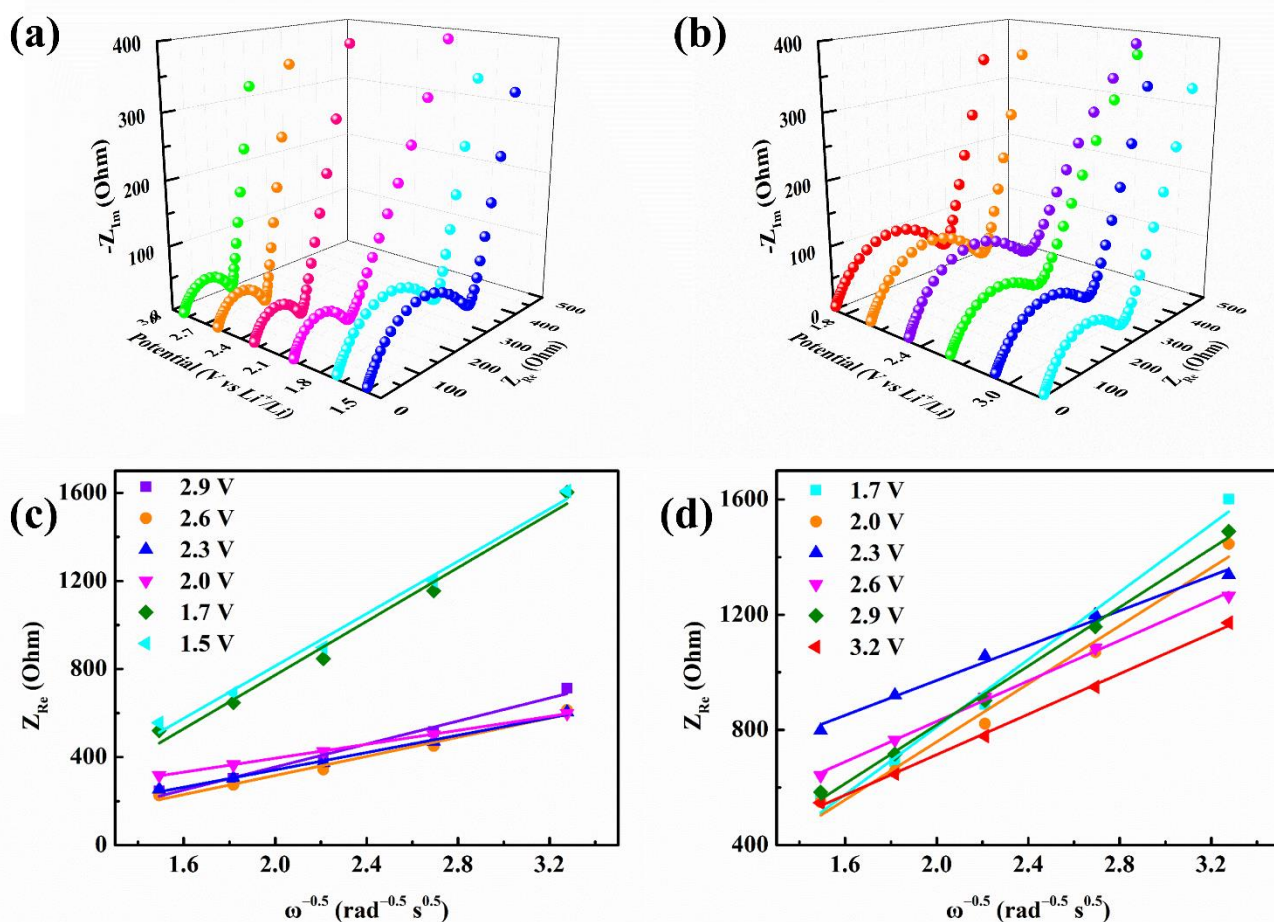


Figure S10 (a, b) EIS spectra and (c, d) corresponding linear relationship between Z_{Re} and $\omega^{-0.5}$ at various states of discharge/charge of DAP.

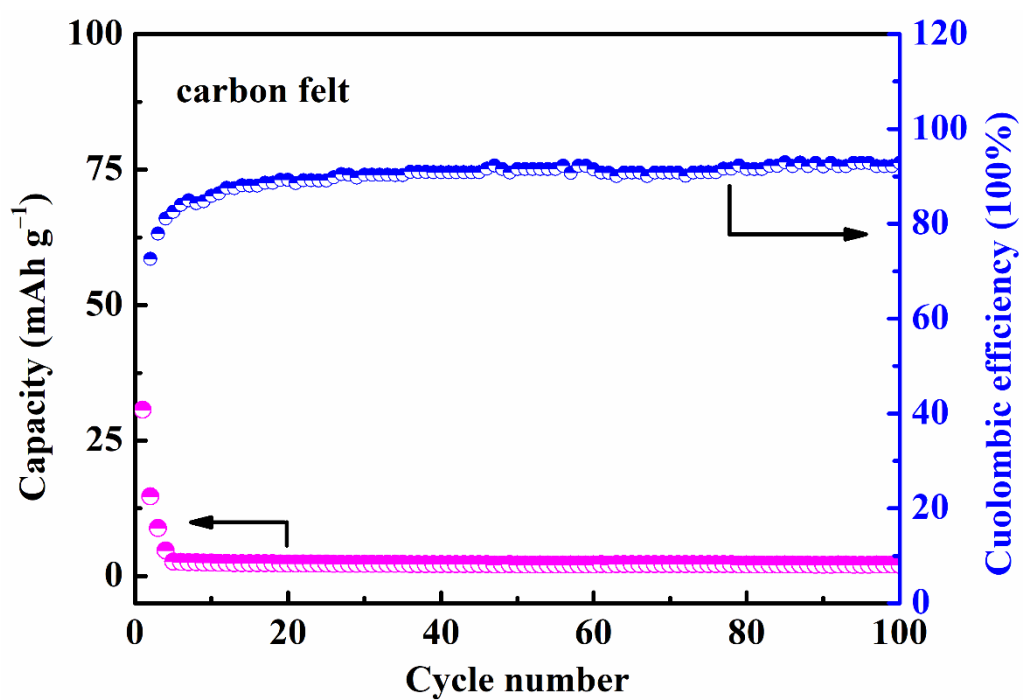


Figure S11 Cycling performance of carbon felt at 0.1 A g⁻¹.

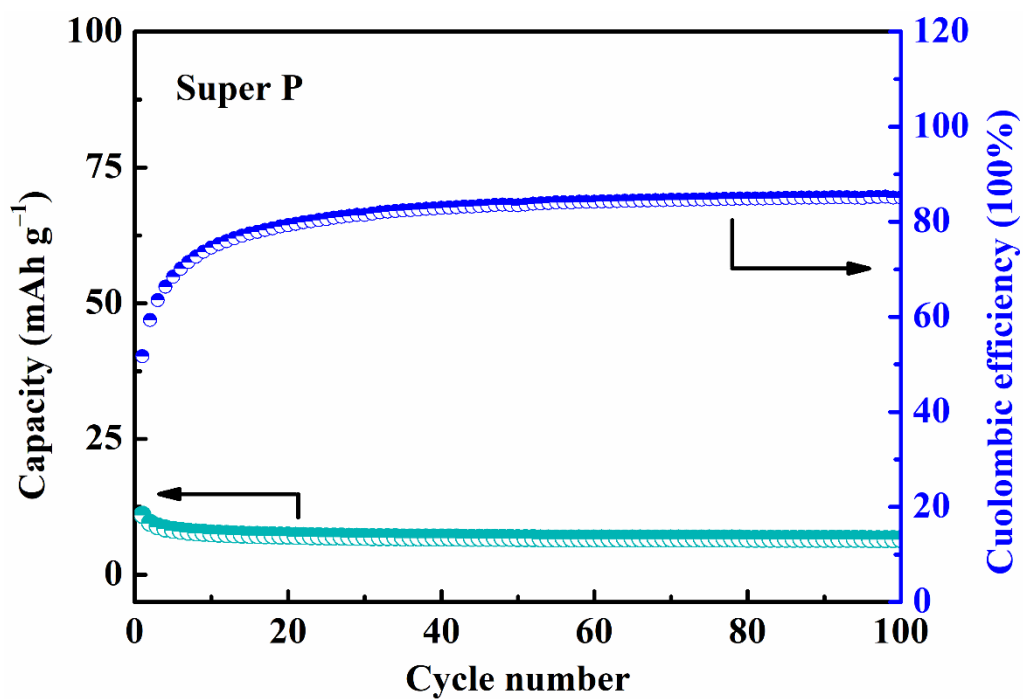


Figure S12 Cycling performance of Super P electrode (Super P: binder = 4:1 wt %) at 0.1 A g⁻¹.

Table S1 Apparent lithium-ion diffusion coefficients of DAP and DAP@C.

	DAP@C	DAP
O1	$1.118 \times 10^{-12} \text{ cm}^2 \text{ s}^{-1}$	$3.704 \times 10^{-13} \text{ cm}^2 \text{ s}^{-1}$
R1	$1.599 \times 10^{-12} \text{ cm}^2 \text{ s}^{-1}$	$3.492 \times 10^{-13} \text{ cm}^2 \text{ s}^{-1}$
O2	/	$3.087 \times 10^{-13} \text{ cm}^2 \text{ s}^{-1}$
R2	/	$2.617 \times 10^{-13} \text{ cm}^2 \text{ s}^{-1}$

Table S2 Calculation of DAP lithium insertion sites.

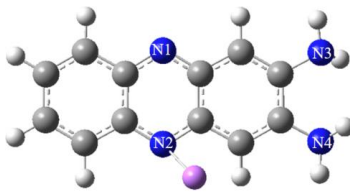
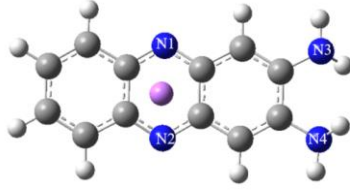
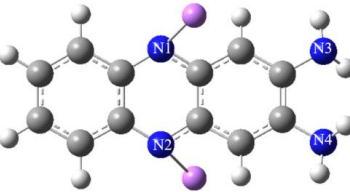
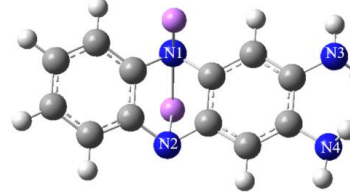
DAP-Li	Structure		
	Energy	most stable	+0.1764 eV
DAP-2Li	Structure		
	Energy	most stable	+0.2309 eV

Table S3 NBO charge of N atoms.

	N1	N2	N3	N4
DAP	-0.40132	-0.40645	-0.89907	-0.92311
DAP ²⁻	-0.63643	-0.64364	-0.90618	-0.9221
DAP-2Li	-0.752	-0.75183	-0.90191	-0.90204

Table S4 Summary of electrochemical performance of DAP.

Active material (anode//cathode)	Electrolyte	Initial capacity (mAh g ⁻¹)@ Current density (mA g ⁻¹)	Capacity retention @Cycle numbers	Reference
Li//DAP@C	1 M LiPF ₆ in EC/DMC=1:1	252@100	66.7% @100	This work
Li//DAP	1 M LiTFSI in DOL/DME=1:1	270@1000	26.7% @100	[1]
Li//DAP	1 M LiTFSI in DOL/DME=1:1	275@100	86% @100	[1]
Zn//DAP	2 M ZnSO ₄ in H ₂ O	210@20	13.3% @200	[2]
Zn//DAP	3 M Zn(CF ₃ SO ₃) ₂ in H ₂ O	144.5@25500	80% @10000	[3]

References

- [1] B. Tian, Z. Ding, G.-H. Ning, W. Tang, C. Peng, B. Liu, J. Su, C. Su, K.P. Loh, Amino group enhanced phenazine derivatives as electrode materials for lithium storage, *Chem. Commun.*, 2017, 53, 2914-2917. <https://doi.org/10.1039/c6cc09084b>
- [2] Q. Wang, Y. Liu, P. Chen, Phenazine-based organic cathode for aqueous zinc secondary batteries, *J. Power Sources*, 2020, 468, 228401. <https://doi.org/10.1016/j.jpowsour.2020.228401>
- [3] J. Liang, M. Tang, L. Cheng, Q. Zhu, R. Ji, X. Liu, Q. Zhang, H. Wang, Z. Liu, 2,3-diaminophenazine as a high-rate rechargeable aqueous zinc-ion batteries cathode, *J. Colloid. Interface Sci.*, 2022, 607, 1262-1268. <https://doi.org/10.1016/j.jcis.2021.09.072>